Oblique Semi-Guided Waves: 2-D Integrated Photonics with Negative Effective Permittivity

(Invited Paper)

Manfred Hammer, Lena Ebers, Andre Hildebrandt, Samer Alhaddad, Jens Förstner
Theoretical Electrical Engineering, Paderborn University, Paderborn, Germany
E-mail: manfred.hammer@uni-paderborn.de

Abstract—Semi-guided waves confined in dielectric slab waveguides are being considered for oblique angles of propagation. If the waves encounter a linear discontinuity of (mostly) arbitrary shape and extension, a variant of Snell's law applies, separately for each pair of incoming and outgoing modes. Depending on the effective indices involved, and on the angle of incidence, power transfer to specific outgoing waves can be allowed or forbidden. In particular, critical angles of incidence can be identified, beyond which any power transfer to non-guided waves is forbidden, i.e. all radiative losses are suppressed. In that case the input power is carried away from the discontinuity exclusively by reflected semi-guided waves in the input slab, or by semi-guided waves that are transmitted into other outgoing slab waveguides. Vectorial equations on a 2-D cross sectional domain apply. These are formally identical to the equations that govern the eigenmodes of 3-D channel waveguides. Here, however, these need to be solved not as an eigenvalue problem, but as an inhomogeneous problem with a right-hand-side that is given by the incoming semi-guided wave, and subject to transparent boundary conditions. The equations resemble a standard 2-D Helmholtz problem, with an effective permittivity in place of the actual relative permittivity. Depending on the properties of the incoming wave, including the angle of incidence, this effective permittivity can become locally negative, causing the suppression of propagating outgoing waves. A series of high-contrast example configurations are discussed, where these effects lead to — in some respects — quite surprising transmission characteristics.

I. INTRODUCTION

In a context of theoretical integrated optics/photonics, spatially two-dimensional models of scattering problems usually refer to a situation, where both the structure under study as well as the solutions sought for the optical electromagnetic fields are constant along one Cartesian coordinate axis. One then obtains the familiar decoupled, TE- and TM-polarized solutions, each governed by a scalar wave- or Helmholtz-type equation. Referring to the setting of Fig. 1, this corresponds to an angle of incidence $\theta = 0°$, i.e. to normal wave incidence. These incoming waves are confined by the slab core in the direction (here x) normal to the slab, but show the functional dependence of a standard harmonic plane wave in the coordinate plane (here y-z) of the slab. Hence we shall use the term "semi-guided waves" to characterize these types of fields.

For this overview paper we will consider a situation, where, for the same structure, the semi-guided waves come in towards the "discontinuity", the central region of interest (darker shading in Fig. 1), at oblique angles of propagation. Fairly general considerations based on the modal properties of the connecting slab waveguides lead to relations between the effective indices and propagation angles of the pairs of
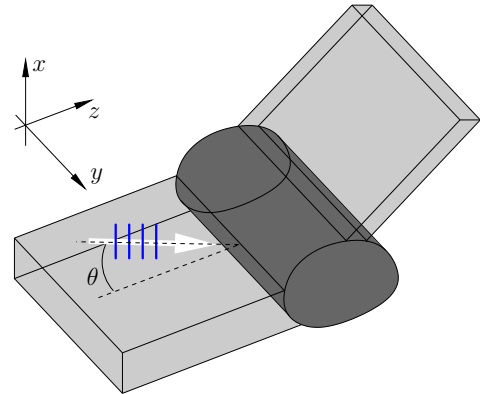

Fig. 1. Schematic illustration of a general "discontinuity" of slab waveguides as discussed in this paper. We use Cartesian coordinates x, y, z; the entire structure is assumed to be homogeneous and infinitely extended along the y-axis. The inner region of interest, the central irregular cylinder (darker shading) is connected to one or more slab waveguides, with in principle arbitrary orientation and position in the x-z-plane. The structure is excited by a semi-guided wave, given by the guided mode supported by one of these connecting slabs, here with x-dependent profile, and with the functional shape of a plane wave, propagating in the y-z plane at an angle θ with respect to the cross section of the central cylinder.

modes that participate in the scattering process. These can be given in the form of Snell's law [1], [2]. In particular, critical angles of incidence can be identified, above which power transfer to specific outgoing waves is suppressed. We review that theory in Section II. A brief look to the formal vectorial equations in Section II-A shows that these effects can be viewed as originating from an effective, angle-dependent permittivity which can become negative.

Our list of illustrating examples in Section III covers a recipe for the quasi-lossless excitation of a thin silicon slab [3], corner- and step-like structures for the transfer of optical power between guiding layers at different levels in a context of silicon photonics [4], [5], and the oblique resonant excitation of a dielectric strip, which might be viewed as a way to realize what is currently discussed as "bound states in a continuum" (BICs) [6]. Further configurations that belong in this context are step-shaped optical folds based on air-clad slab waveguides [7], the spiral modes supported by bent slab waveguides [8], which also play a role in corner- and step-structures with rounded edges [9], and differentiators and integrators for semi-guided beams [10]. Note that with the present theory we take up early concepts of integrated optics [11], [12], where also the propagation of semi-guided waves in dielectric slabs has been considered, applying models of free-space optics to the in-

plane propagation. Here, however, we focus on examples with substantial refractive index contrast, where the effects related to the oblique propagation (loss suppression, critical angles, and intervals between them) are much more pronounced.

II. SLAB WAVEGUIDE DISCONTINUITIES AT OBLIQUE INCIDENCE

Following largely the arguments of Ref. [2], [5], we start with the general "discontinuity" of Fig. 1, introduced in some more detail in Fig. 2. One discerns the slab that supports the incoming and potential reflected waves, further slabs that support outgoing waves, and a central region of interest. In case of the examples of Section III, that region covers the waveguide interfaces, and the intermediate segment (Fig. 3), a cylinder including the corner- and step-discontinuities (Fig. 4), and the strip and an adjoining slab segment (Fig. 5). Cartesian coordinates are oriented such that the entire structure is constant along the y-axis with the z-coordinate along the axis of the incoming waveguide.
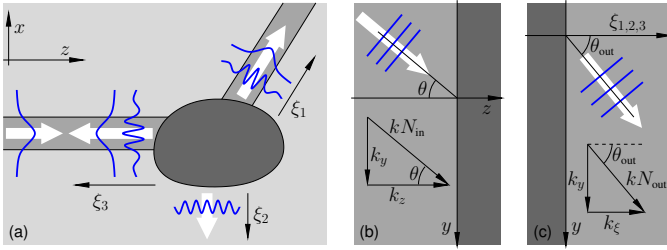

Fig. 2. Cross section view (a) of the slab waveguide discontinuity of Fig. 1. Further panels show top views of the input waveguide (b), and generic "top views" of any of the output slabs (c). The incoming wave propagates with effective mode index N_{in} at angle θ in the y-z-plane, with an x-dependent mode profile. Outgoing waves with effective mode indices N_{out} propagate at angles θ_{out} in the y-ξ-planes, where ξ is some suitable local coordinate along the slab core in the x-z-cross-sectional plane.

We consider time harmonic fields $\sim \exp(\mathrm{i}\omega t)$ with angular frequency $\omega = kc = 2\pi c/\lambda$, for vacuum wavelength λ, wavenumber k and speed of light c. As shown schematically by Fig. 2(b), the incoming field is a polarized guided mode supported by the input slab, with vectorial profile $\mathbf{\Psi}_{\text{in}}(k_y; x)$ and effective mode index N_{in} (cf. Refs. [2], [13]), propagating at angle θ in the y-z-plane. This relates to a functional dependence

$$\sim \mathbf{\Psi}_{\text{in}}(k_y, x) \exp(-\mathrm{i}(k_y y + k_z z)), \qquad (1)$$

with

$$k_y = k N_{\text{in}} \sin \theta, \qquad (2)$$

$k_z = k N_{\text{in}} \cos \theta$, and $k_y^2 + k_z^2 = k^2 N_{\text{in}}^2$. The entire problem is homogeneous along y. Therefore the global solution can be restricted to the single spatial Fourier component k_y of the incident wave: The harmonic y-dependence of Eq. (1) is imposed on all optical electromagnetic fields, at all positions. According to Eq. (2), for a specific incident mode with given N_{in}, the wavenumber k_y can be specified by the angle of incidence θ.

Next we select one outgoing mode with profile $\mathbf{\Psi}_{\text{out}}$ and effective index N_{out}. According to Fig. 2(a), this can be a guided mode supported by one of the slabs with coordinates

ξ_1 or $\xi_3 = -z$. What follows, however, applies just as well to some non-guided, radiated wave propagating in the y-ξ_2-plane (in a homogeneous half-space). Analogously to Eq. (1), the outgoing field (cf. Fig. 2(c) can be written

$$\sim \mathbf{\Psi}_{\text{out}}(k_y, \, . \,) \exp(-\mathrm{i}(k_y y + k_\xi \xi)), \qquad (3)$$

where the wave equation [2] requires that

$$k^2 N_{\text{out}}^2 = k_y^2 + k_\xi^2 \qquad (4)$$

holds for the cross-sectional wavenumber k_ξ, still with the common wavenumber (2) given by the incoming field. Eq. (4) determines the propagation character of that particular outgoing mode, i.e. decides whether, for a real wavenumber k_ξ, the wave is propagating along ξ, or, for imaginary k_ξ, the mode becomes evanescent in direction ξ.

Depending on the angle of incidence one thus has to distinguish two cases. For a sufficiently large effective mode index N_{out} with $k^2 N_{\text{out}}^2 > k_y^2$, the outgoing field propagates at an angle θ_{out} with wavenumber $k_\xi = k N_{\text{out}} \cos \theta_{\text{out}}$. The effective indices of the incoming and outgoing modes, and the angles of incidence and refraction, satisfy a relation that can be given the form of Snell's law:

$$N_{\text{out}} \sin \theta_{\text{out}} = N_{\text{in}} \sin \theta. \qquad (5)$$

Hence, depending on the properties of the slab waveguides involved, different outgoing waves are thus observed each at its own specific angle.

An outgoing mode with smaller effective mode index N_{out}, however, with $k^2 N_{\text{out}}^2 < k_y^2$, becomes evanescent with an imaginary wavenumber $k_\xi = -\mathrm{i}\sqrt{k_y^2 - k^2 N_{\text{out}}^2}$. These waves decay with growing distance ξ in the cross section plane. While they may well contribute significantly to the overall field in a region close to the discontinuity, these evanescent outgoing fields *do not carry optical power* [14] away from this central inner region.

When increasing the angle of incidence θ, starting from normal incidence $\theta = 0$, a mode's type can thus change from ξ-propagating to ξ-evanescent. This occurs, for an outgoing mode with effective index $N_{\text{out}} < N_{\text{in}}$, if $k^2 N_{\text{out}}^2 = k^2 N_{\text{in}}^2 \sin^2 \theta$. Hence, for each pair of input and output modes, one can define a characteristic angle θ_{cr} with

$$\sin \theta_{\text{cr}} = N_{\text{out}}/N_{\text{in}} \qquad (6)$$

such that the outgoing mode does not carry power, if the input wave arrives at an angle of incidence $\theta > \theta_{\text{cr}}$ beyond that critical angle.

The example configurations in Section III are based on symmetric slab waveguides with core- and cladding-refractive indices n_{g} (guiding regions) and n_{b} (background). The structures are excited by the fundamental TE mode of the input slab. Its effective mode index $N_{\text{in}} = N_{\text{TE0}}$ exceeds that of the fundamental TM mode N_{TM0}. Both values are between the core and cladding refractive indices $n_{\text{g}} > N_{\text{TE0}} > N_{\text{TM0}} > n_{\text{b}}$. Following the former arguments one can then conclude [5]:

- All modes of the connecting waveguides (also of those "without core", cf. coordinate ξ_2 in Fig. 2(a)) that relate to radiative waves, with oscillatory behavior in

the cladding regions ("cladding modes"), have effective indices below the upper limit n_b of the radiation continuum. Their characteristic angles (6) are smaller than the critical angle θ_b, defined by $\sin\theta_b = n_b/N_{TE0}$, associated with the background refractive index. Consequently *all radiation losses vanish for incidence at angles $\theta > \theta_b$.*

- All TM polarized modes supported by these waveguides have effective mode indices below N_{TM0} (assuming the input slab to be the one with the largest thickness, which is the case for all our examples). Their characteristic angles (6) are thus smaller than the critical angle θ_m, defined by $\sin\theta_m = N_{TM0}/N_{TE0}$, associated with the fundamental TM wave. Consequently, *for incidence at angles $\theta > \theta_m$, all incoming optical power is carried away by outgoing guided TE waves.*

Note that these arguments rely solely on the modal properties (1), (3) of the access waveguides, irrespectively of their orientation and positioning. The reasoning applies to configurations with — in principle — arbitrary interior and arbitrary extension of the region that connects the slab waveguide outlets.

Similar rationales have been applied to problems of plane-wave scattering from cylinders at oblique incidence [15], [16], to slab waveguides with straight discontinuities (end facets), for oblique incidence of guided modes [1], [13], [17], [18], and to periodically corrugated slab waveguides [19], [20].

A. Formal problem

To complement these general considerations, we comment briefly on the rigorous differential equations that govern the problems at hand [1], [2]. The Maxwell curl equations in the frequency domain apply, for the electric field $\tilde{E}$ and magnetic field $\tilde{H}$, for uncharged dielectric, nonmagnetic linear media with relative permittivity $\epsilon = n^2$, for vacuum permittivity ϵ_0 and permeability μ_0:

$$\text{curl}\,\tilde{E} = -\mathrm{i}\omega\mu_0\tilde{H}, \qquad \text{curl}\,\tilde{H} = \mathrm{i}\omega\epsilon\epsilon_0\tilde{E}. \tag{7}$$

The structures under consideration are y-homogeneous, $\partial_y\epsilon = 0$. Correspondingly, the electromagnetic fields exhibit a harmonic y-dependence

$$\begin{pmatrix} \tilde{E} \\ \tilde{H} \end{pmatrix}(x,y,z) = \begin{pmatrix} E \\ H \end{pmatrix}(x,z)\,\exp(-\mathrm{i}k_y y) \tag{8}$$

with the wavenumber (2) given by the incident wave.

These prerequisites lead to a system of vectorial equations on the x-z-cross section plane, parameterized by k_y. These are formally identical to the equations that govern the hybrid eigenmodes of 3-D dielectric channel waveguides (with 2-D cross sections) [21]; the given wavenumber k_y takes the place of the propagation constant (eigenvalue) of the channel mode. In the present case, however, these equations need to be solved as a nonhomogeneous problem with the incoming wave as a right-hand side, with boundary conditions that can accommodate the given influx, and that are transparent for outgoing guided and nonguided waves.

In regions with locally constant permittivity $\partial_x\epsilon = \partial_z\epsilon = 0$, the vectorial equations shrink to the scalar Helmholtz equation

$$\left(\partial_x^2 + \partial_z^2\right)\phi + k^2\epsilon_{\text{eff}}\phi = 0, \tag{9}$$

valid separately for all components $\phi = E_j, H_j$ of the optical electromagnetic fields, with the angle-dependent effective permittivity

$$\epsilon_{\text{eff}}(x,z) = \epsilon(x,z) - N_{\text{in}}^2\sin^2\theta. \tag{10}$$

Oblique excitation at an angle θ beyond the critical angle θ_b then leads to a negative local effective permittivity (10), and consequently to evanescent wave propagation, in the cladding regions with refractive index n_b. Hence the suppression of radiative losses can be understood just as well in terms of this negative effective permittivity [1].

Apart from these limiting arguments, in general numerical methods are required to obtain actual quantitative solutions for the 2-D vectorial problem of Eqs. (7), (8).

III. COMPUTATIONAL EXAMPLES

The results of Sections III-A–III-C are generated with two types of numerical techniques. A quasi-analytical solver, based on a rigorous vectorial expansion into 1-D eigenmodes along both of the cross section coordinates (vectorial quadridirectional eigenmode expansion, vQUEP, [2], [22], [23]) appears to be robust, accurate, and comparably efficient for these type of problems. It is however limited to strictly rectangular configurations.

Alternatively, the finite-element solvers included in the COMSOL multiphysics suite [24] cover these parameterized 2-D problems as well. Arbitrary permittivity profiles can be represented adequately, in principle; some issues related to the performance of transparent boundary conditions in cases of inhomogeneous exterior were observed (high-contrast waveguides cross the boundaries), in particular in cases where the waves leave the computational domain at shallow angles. The results on structures with rounded edges in Refs. [8], [9] are based on those solvers; for the following examples, the COMSOL suite has been used for a (partial) corroboration of the vQUEP results.

A. Quasi-lossless excitation of a thin silicon slab waveguide

In a traditional 2-D setting, guided waves traversing an abrupt interface between different slab waveguides typically generate more or less pronounced reflections and scattering losses. High-contrast silicon slabs are considered, as introduced Fig. 3(a), for the parameters given in the caption. The field of Fig. 3(b) relates to the standard setting, with normal incidence of the guided TE wave on the abrupt interface between the slabs with thicknesses d and r. One observes a reflectance of $R = 9\%$ and about 15% of radiation losses.

We now investigate what happens if the fundamental TE mode of the thicker segment comes in at the junction at oblique angles. Mode analysis of the two slab regions [25] shows that both slabs support a fundamental TE- and TM-mode each. The reasoning of Section II then predicts critical angles of incidence $\theta_b = 30.9°$ for outgoing radiation in the cladding, $\theta_{T,TM} = 31.2°$, $\theta_{T,TE} = 37.7°$ for the guided TM and TE modes of the thin slab, and $\theta_{R,TM} = 46.3°$ for the
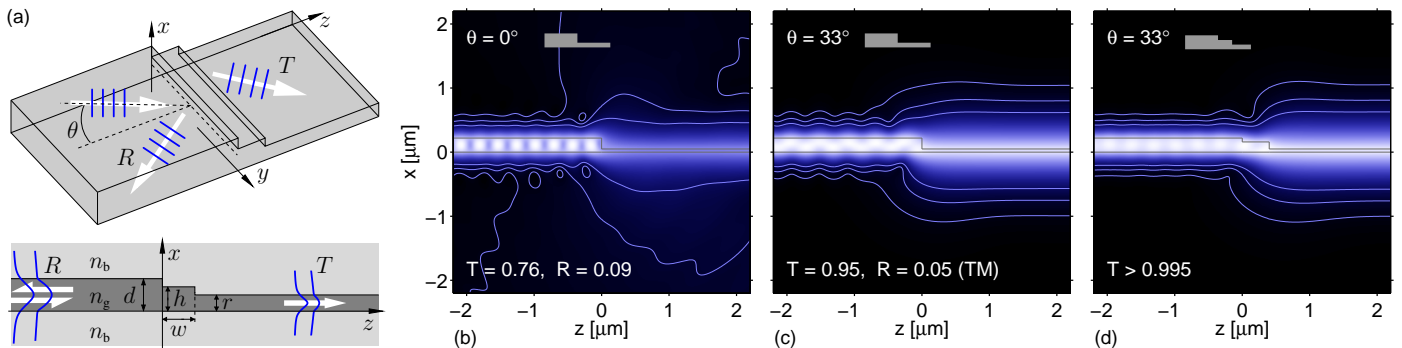
Fig. 3. Artists impression and cross section view (a) of the waveguide interface. Single-mode Si/SiO$_2$-waveguides of thicknesses $d = 0.22\,\mu m$ and $r = 0.05\,\mu m$ are considered, with refractive indices $n_g = 3.45$ and $n_b = 1.45$, at a wavelength of $1.55\,\mu m$. Transmittances T and reflectances R are given for semi-guided TE excitation at angle θ. Results for abrupt interfaces at normal (b) and oblique incidence (c), and for a "coated" interface (d), with a segment of height $h = 0.16\,\mu m$ and width $w = 0.4\,\mu m$, are shown. The plots relate to the absolute magnetic field $|\boldsymbol{H}|$ in the x-z cross section plane, with contours at 2%, 5%, and 10% of the maximum levels. [3]

reflection into the guided TM mode of the input slab. Aiming at a high transmission to the TE wave of the thin slab, we thus switch to an angle of incidence between θ_b and $\theta_{T,TE}$, such that radiation losses are suppressed, while the thin slab still supports a propagating guided TE mode. For a somewhat arbitrarily chosen angle of $\theta = 33°$, it turns out that the TE transmittance of 95% actually exceeds the level for normal incidence. The waves, however, are still partly reflected, mainly into the backwards TM mode. Fig. 3(c) gives an impression of the corresponding field.

Motivated by the traditional technique of reflection suppression, we introduce a short waveguide segment of intermediate thickness at the former interface, emulating a "layer" of a certain thickness with intermediate (here effective) refractive index. Optimization of the transmittance through varying the height and width of that segment (not shown) leads to the configuration of Fig. 3(d) with a guided-wave TE-to-TE transmittance above 99.5%. We have thus realized what one might call an "anti-reflection-coating" in an integrated optics setting.

B. Corner- and step-like folds in planar dielectric slabs

Concepts for the 3-D integration of optical devices [26], [27] are at present discussed in particular in the field of silicon photonics [28], [29]. We look at the task to enable an optical connection, a "via", between guiding layers at different vertical levels of an integrated optical chip, in this context of high-contrast waveguides.

To that end, we first consider a structure of corner shape, as in Fig. 4(a), that might be expected to redirect some of the guided input from the horizontal to the vertical layer. As to be expected, in a conventional 2-D setting with normal incidence of the guided TE slab mode, our solvers predict a moderate performance with a TE-reflectance of $R_{TE} = 13\%$ and transmittance of $T_{TE} = 14\%$, i.e. with substantial losses. Fig. 4(b) shows the related field.

Applying the reasoning of Section II, we now consider oblique wave incidence at varying angles θ. The symmetric slab waveguides (horizontal and vertical slabs are of the same thickness) with the parameters as given in the caption of Fig. 4 support fundamental TE- and TM waves only [25]. One obtains the critical angles $\theta_b = 31°$ for outgoing non-guided waves,

and $\theta_{TM} = 46.3°$ for the scattering to reflected or upwards transmitted guided TM waves.

With the aim of avoiding radiation losses, we thus select the range of angles of incidence beyond θ_b. Fig. 4(c) illustrates the optical field at an angle of $\theta = 36.5°$. Here the solvers predict large, almost purely TE-polarized reflection $R_{TE} = 26\%$, $R_{TM} = 1\%$, and a substantial level of polarization conversion with transmittances $T_{TE} = 10\%$, and $T_{TM} = 63\%$. The TM transmittance reaches a maximum at this angle [4]. Increasing the angle of incidence further beyond θ_{TM}, the conversion to TM polarized waves is suppressed. At $\theta = 64°$ the TE transmittance $T_{TE} = 32\%$ is at maximum, with the remainder of the incident power carried by the reflected fundamental TE mode.

After having passed the first corner, the waves need to be channelled into the horizontal direction again. By adding another, identical corner fold, we arrive at the step structure of Fig. 4(e). We adopt the configuration of Fig. 4(d) with maximum TE transmittance, at $\theta = 64°$. Radiation losses are suppressed, and guided TM wave become evanescent for this angle. This holds for the separate corners, but just as well for the entire step. Assuming a sufficient step height such that evanescent waves don't play a role, only the upward and downward propagating guided TE waves contribute to the power transfer in the vertical waveguide segment between both corners.

The step system can thus be viewed as a configuration akin to a Fabry-Perot-interferometer, where the corners work as partial reflectors. By varying the height of the vertical waveguide segment [4], one identifies step-like configurations that transmit the semi-guided plane waves without radiation losses, and virtually without reflections, at specific angles of incidence, where the transmission resonances of the Fabry-Perot system are realized.

The panels of Fig. 4(f, g) show exemplary fields for the step structure, with a vertical separation between the horizontal layers optimized for $\theta = 64°$. At normal incidence $\theta = 0°$ (Fig. 4(f)), for the standard 2-D TE setting, our simulations predict levels of transmittance $T = 3\%$ and reflectance $R = 11\%$, with the entire remainder of the incident power lost to radiation. Within the numerical error margins, this
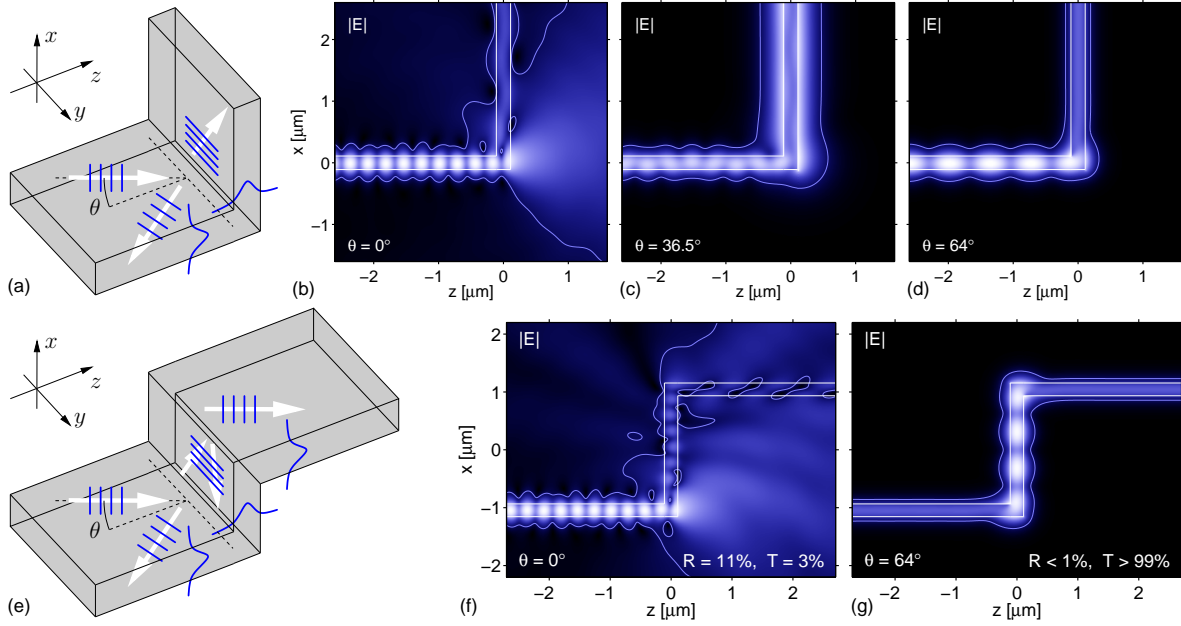
Fig. 4. Oblique incidence of semi-guided waves on corner- and step-shaped folds of slab waveguides, schematic (a, e), and cross-section views of the optical electric field (absolute value $|\boldsymbol{E}|$, contour at 10% of the field maximum). Parameters: refractive indices 3.45 (slab cores) : 1.45 (cladding), thickness of horizontal and vertical slabs 220 nm, vertical distance between the upper and lower interfaces of the lower and upper layers $1.868\,\mu$m, incidence of semi-guided TE polarized waves at $\lambda = 1.55\,\mu$m. [4]

changes to perfect performance $T > 99\%$, $R < 1\%$ with full transmission at $\theta = 64°$. Accordingly, the field in Fig. 4(g) exhibits the purely forward wave in the horizontal input- and output waveguides, and a resonant pattern of partly standing waves in the vertical segment.

C. An open dielectric cavity with infinite Q

Dielectric optical cavities, if based on internal reflection (as opposed to periodically corrugated regions, i.e. photonic crystals), are always deemed to be inherently lossy. Among many other concepts, we here look at dielectric cavities of rectangular shape. In a standard 2-D setting, specific dimensioning is required to obtain a small resonator cavity with even moderate quality factor [30]–[32]. The structures discussed there are very similar to the configuration introduced in Fig. 5(a,b). A dielectric strip of — within limits — arbitrary width and height is placed at some distance on top of a slab waveguide. The strip constitutes the cavity that is excited, here potentially at oblique angles, by semi-guided waves in the slab, which thus works as our bus waveguide.

Similar configurations have been investigated in the literature, for other purposes. Among the related proposals are devices for the differentiation and integration of semi-guided beams [10] (the structure of Fig. 5(a,b) with a strip/rib that rests directly on the substrate), a setting for the observation of lateral whispering gallery resonances at angled crossings of optical fibers [33], or interferometer concepts based on semi-guided waves passing a multimode rib segment at normal incidence, for application as polarizers [14] or isolators [34].

The analysis starts with computing the guided mode of the dielectric strip. At a vacuum wavelength of $\lambda = 1.55\,\mu$m, COMSOL predicts a fundamental guided TE-like hybrid mode

with effective index $N_{\mathrm{m}} = 2.4192$ (further modes are supported). In line with the discussion of Section II, this can be translated to an angle of incidence θ_{m} with $kN_{\mathrm{m}} = kN_{\mathrm{TE0}} \sin\theta_{\mathrm{m}}$ of $\theta_{\mathrm{m}} = 58.99°$. We can thus expect to find a resonance, if the strip is excited at an angle of incidence close to θ_{m}. A respective sweep over θ shows that this is indeed the case; the panels of Fig. 5(c–e) illustrate some corresponding fields. In an off resonance state (c), the wave just passes by underneath the strip, with hardly any disturbance. At half resonance (b), determined by a reflectance $R = 50\%$, a stronger field is observed in the strip. At resonance, the field in the strip reaches a maximum, and the strip generates a reflectance of $R = 100\%$. All these angles of incidence are beyond the critical angle for radiation into the cladding areas; radiation losses are thus fully suppressed.

Since the cavity itself does not show any radiation losses, the resonance characteristics are determined solely by the strength of the interaction with the bus waveguide, i.e. by the gap distance g. For increasing gap, we observe that the resonance angle tends to the value θ_{m} as given by the rib mode. This is accompanied by a narrowing angular width of the resonance, and correspondingly a growing field strength in the rib. At the same time the "height" of the resonance peak, the maximum reflectance at the resonance angle, remains at unity. Simulations carried out so far, and the extremal values observed, are merely limited by the accuracies of the solvers available.

Similar features can be observed when varying the vacuum wavelength, if the angle of incidence is fixed at the level θ_{m}. The resonance then appears at the vacuum wavelength $\lambda = 1.55\,\mu$m. Also in that case, for increasing g, the resonance wavelength tends to the value of $1.55\,\mu$m as given by the rib mode. One finds a narrowing spectral width of the resonance,
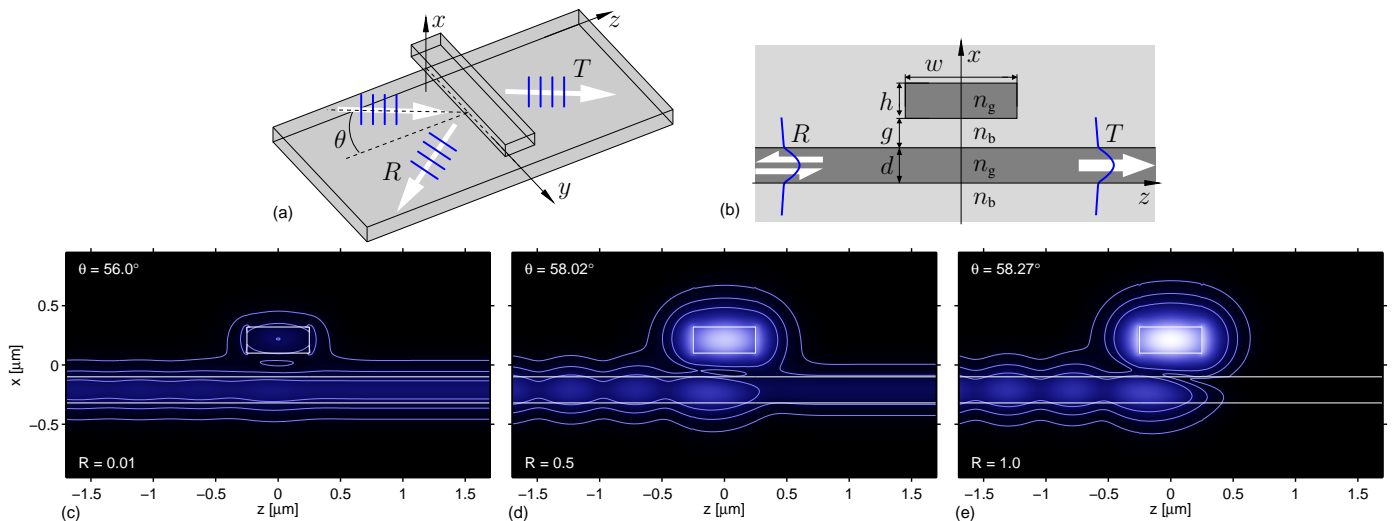
Fig. 5. Oblique evanescent excitation of a dielectric strip, schematic (a), and cross section view (b). Panels (c–e) show the absolute electric field $|\boldsymbol{E}|$ on the x-z-cross section plane, for angles of incidence $\theta = 56°$ (c, off resonance), $\theta = 58.02°$ (c, at "half maximum" of the resonance), and $\theta = 58.27°$ (c, at resonance). Color levels of the panels are comparable; the contours indicate the levels of 2%, 5%, and 10% of the overall field maximum. Parameters: refractive indices $n_g = 3.45$ (guiding regions), $n_b = 1.45$ (substrate, gap layer, and cladding), slab thicknesses $d = h = 0.22\,\mu\text{m}$, strip width $w = 0.5\,\mu\text{m}$, gap $g = 0.2\,\mu\text{m}$, TE excitation at vacuum wavelength $\lambda = 1.55\,\mu\text{m}$.

with exponentially increasing Q-factor, and correspondingly a growing field enhancement in the rib. Also here the maximum reflectance at the resonance wavelength, remains at unity.

Accepting that setting with fixed angle of incidence and variable vacuum wavelength / frequency, for a configuration with *large* distance g, this would be a way to realize a system with a nonradiating bound state (the rib mode) and a wave continuum (the waves supported by the slab) in a range of frequencies that cover the (real) eigenfrequency of the bound state, i.e. an explicitly simple way to realize what might be termed a "bound state in a continuum" [6], [35]–[37]. Note that, in a context of photonics, these BICs are most frequently discussed in a framework of specifically tailored periodic structures / of photonic crystals. Perhaps, due to the spatial separation of the localized strip mode and continuum of waves in the slab waveguide, here the notion of a "bound state coupled to a continuum" might be more adequate.

IV. CONCLUDING REMARKS

With the "2-D problems with oblique incidence" we reconsider older concepts of integrated optics that appear to have largely been neglected over the more recent past. It turns out that, if transferred to present high contrast platforms (typically silicon photonics), the related phenomena can be observed at rather moderate angles of incidence (i.e. not only at grazing incidence). This offers options for the realization of a series of partly astonishing functionalities, in exceptionally simple configurations. Some examples have been shown in this paper; more is expected to come.

For the present paper, we restricted the discussion to solutions generated by incoming semi-guided plane waves with a single, well-defined angle of incidence. As shown in Refs. [5], [9], [10], suitable superpositions of these solutions can be prepared that relate to the oblique incidence of still semi-guided, but now laterally confined "beams". Gaussian

superpositions have been considered [5], [10], as well as wave bundles excited by incoming rib waveguides with shallow etching [9]. The incoming wave-packets then cover a range of angles of incidence, where a narrow angular range corresponds to an incoming bundle of large (y-) extension. For those of the former examples that do not rely critically on resonance effects (such as the reflection-coated transition, Section III-A, or the 90°-edges, Section III-B), transmission properties close to the results as shown here are obtained. The configurations where narrow resonances play a role (the step structure, Section III-B, and the strip-resonator of Section III-C), however, require wide, spectrally narrow incoming bundles to exhibit the transmission characteristics as discussed.

ACKNOWLEDGMENTS

REFERENCES

[1] F. Çivitci, M. Hammer, and H. J. W. M. Hoekstra, "Semi-guided plane wave reflection by thin-film transitions for angled incidence," *Optical and Quantum Electronics*, vol. 46, no. 3, pp. 477–490, 2014.

[2] M. Hammer, "Oblique incidence of semi-guided waves on rectangular slab waveguide discontinuities: A vectorial QUEP solver," *Optics Communications*, vol. 338, pp. 447–456, 2015.

[3] M. Hammer, L. Ebers, and J. Förstner, "Oblique quasi-lossless excitation of a thin silicon slab waveguide," XXVI International Workshop on Optical Wave & Waveguide Theory and Numerical Modeling, Bad Sassendorf, Germany, 2018, book of abstracts, 35 (2018).

[4] M. Hammer, A. Hildebrandt, and J. Förstner, "How planar optical waves can be made to climb dielectric steps," *Optics Letters*, vol. 40, no. 16, pp. 3711–3714, 2015.

[5] M. Hammer, A. Hildebrandt, and J. Förstner, "Full resonant transmission of semi-guided planar waves through slab waveguide steps at oblique incidence," *Journal of Lightwave Technology*, vol. 34, no. 3, pp. 997–1005, 2016.

[6] C. W. Hsu, B. Zhen, A. D. Stone, J. D. Joannopoulos, and M. Soljačić, "Bound states in the continuum," *Nature Reviews Materials*, vol. 1, p. 16048, 2016.

[7] A. Hildebrandt, S. Alhaddad, M. Hammer, and J. Förstner, "Oblique incidence of semi-guided waves on step-like folds in planar dielectric slabs: Lossless vertical interconnects in 3D integrated photonic circuits," in *Proceedings of SPIE*, vol. 9750, 2016, pp. 97 501B–97 501B–7.

[8] L. Ebers, M. Hammer, and J. Förstner, "Spiral modes supported by circular dielectric tubes and tube segments," *Optical and Quantum Electronics*, vol. 49, no. 4, p. 176, 2017.

[9] L. Ebers, M. Hammer, and J. Förstner, "Oblique incidence of semi-guided planar waves on slab waveguide steps: Effects of rounded edges," *Optics Express*, 2018, (submitted for publication).

[10] E. A. Bezus, L. L. Doskolovich, D. A. Bykov, and V. A. Soifer, "Spatial differentiation and integration of optical beams in a slab waveguide by a single dielectric ridge," 2018, arXiv:1804.02267v1 [physics.optics].

[11] P. K. Tien, "Integrated optics and new wave phenomena in optical waveguides," *Reviews of Modern Physics*, vol. 49, no. 2, pp. 361–419, 1977.

[12] R. Ulrich and R. J. Martin, "Geometrical optics in thin film light guides," *Applied Optics*, vol. 10, no. 9, pp. 2077–2085, 1971.

[13] W. Biehlig and U. Langbein, "Three-dimensional step discontinuities in planar waveguides: Angular-spectrum representation of guided wavefields and generalized matrix-operator formalism," *Optical and Quantum Electronics*, vol. 22, no. 4, pp. 319–333, 1990.

[14] M. Lohmeyer and R. Stoffer, "Integrated optical cross strip polarizer concept," *Optical and Quantum Electronics*, vol. 33, no. 4/5, pp. 413–431, 2001.

[15] J. R. Wait, "Scattering of a plane wave from a circular dielectric cylinder at oblique incidence," *Canadian Journal of Physics*, vol. 33, no. 5, pp. 189–195, 1955.

[16] H. Wang and G. Nakamura, "The integral equation method for electromagnetic scattering problem at oblique incidence," *Applied Numerical Mathematics*, vol. 62, no. 7, pp. 860–873, 2012.

[17] S.-T. Peng and A. Oliner, "Guidance and leakage properties of a class of open dielectric waveguides: Part I — mathematical formulations," *IEEE Transactions on Microwave Theory and Techniques*, vol. MTT-29, no. 9, pp. 843–854, 1981.

[18] T. P. Shen, R. F. Wallis, A. A. Maradudin, and G. I. Stegeman, "Fresnel-like behavior of guided waves," *Journal of the Optical Society of America A*, vol. 4, no. 11, pp. 2120–2132, 1987.

[19] K. Wagatsuma, H. Sakaki, and S. Saito, "Mode conversion and optical filtering of obliquely incident waves in corrugated waveguide filters," *IEEE Journal of Quantum Electronics*, vol. 15, no. 7, pp. 632–637, 1979.

[20] J. Van Roey and P. E. Lagasse, "Coupled wave analysis of obliquely incident waves in thin film gratings," *Applied Optics*, vol. 20, no. 3, pp. 423–429, 1981.

[21] C. Vassallo, *Optical Waveguide Concepts*. Amsterdam: Elsevier, 1991.

[22] M. Hammer, "Quadridirectional eigenmode expansion scheme for 2-D modeling of wave propagation in integrated optics," *Optics Communications*, vol. 235, no. 4–6, pp. 285–303, 2004.

[23] M. Hammer, "METRIC — Mode expansion tools for 2D rectangular integrated optical circuits," http://metric.computational-photonics.eu/.

[24] Comsol Multiphysics GmbH, Göttingen, Germany; http://www.comsol.com.

[25] M. Hammer, "OMS — 1-D mode solver for dielectric multilayer slab waveguides," http://www.computational-photonics.eu/oms.html.

[26] P. Prakash Koonath and B. Jalali, "Multilayer 3-D photonics in silicon," *Optics Express*, vol. 15, no. 20, pp. 12 686–12 691, 2007.

[27] N. Sherwood-Droz and M. Lipson, "Scalable 3D dense integration of photonics on bulk silicon," *Optics Express*, vol. 19, no. 18, pp. 17 758–17 765, 2011.

[28] R. Soref, "The past, present, and future of silicon photonics," *IEEE Journal of Selected Topics in Quantum Electronics*, vol. 12, no. 6, pp. 1678–1687, 2006.

[29] P. Koonath, T. Indukuri, and B. Jalali, "Monolithic 3-D silicon photonics," *Journal of Lightwave Technology*, vol. 24, no. 4, pp. 1796–1804, 2006.

[30] C. Manolatou, M. J. Khan, S. Fan, P. R. Villeneuve, H. A. Haus, and J. D. Joannopoulos, "Coupling of modes analysis of resonant channel add-drop filters," *IEEE Journal of Quantum Electronics*, vol. 35, no. 9, pp. 1322–1331, 1999.

[31] M. Lohmeyer, "Mode expansion modeling of rectangular integrated optical microresonators," *Optical and Quantum Electronics*, vol. 34, no. 5, pp. 541–557, 2002.

[32] M. Hammer, "Resonant coupling of dielectric optical waveguides via rectangular microcavities: The coupled guided mode perspective," *Optics Communications*, vol. 214, no. 1–6, pp. 155–170, 2002.

[33] T. A. Birks, J. C. Knight, and T. E. Dimmick, "High-resolution measurement of the fiber diameter variations using whispering gallery modes and no optical alignment," *IEEE Photonics Technology Letters*, vol. 12, no. 2, pp. 182–183, 2000.

[34] M. Lohmeyer, L. Wilkens, O. Zhuromskyy, H. Dötsch, and P. Hertel, "Integrated magnetooptic cross strip isolator," *Optics Communications*, vol. 189, no. 4–6, pp. 251–259, 2001.

[35] D. C. Marinica, A. G. Borisov, and S. V. Shabanov, "Bound states in the continuum in photonics," *Physical Review Letters*, vol. 100, no. 18, p. 183902, 2008.

[36] Z. Hu and L. Y. Y., "Standing waves on two-dimensional periodic dielectric waveguides," *Journal of Optics*, vol. 17, no. 6, p. 065601, 2015.

[37] L. Yuan and Y. Y. Lu, "Bound states in the continuum on periodic structures: perturbation theory and robustness," *Optics Letters*, vol. 42, no. 21, pp. 4490–4493, 2017.